Supplementary Information: Specific effects of monovalent counterions on the structural and interfacial properties of dodecyl sulfate monolayers†

October 18, 2016

Daniel T. Allen,[a] Yussif Saaka,[b], Luis Carlos Pardo,[c] M. Jayne Lawrence,[b] and Christian D. Lorenz,[a*]

1 Force field parameters

Table 1: Force field parameters for counterions

Atom type	ϵ (kcal/mol)	σ (Å)	Partial charge
Li^+	0.00233	2.311882	+1.0
Na^+	0.0469	2.513671	+1.0
Cs^+	0.1900	3.741775	+1.0
N (NH_4^+)	0.2000	3.296325	-0.32
H (NH_4^+)	0.0460	0.400014	+0.33

The force field parameters used for the description of the counterions were taken from the CHARMM36 additive force field. Table 1 displays the parameters for the non-bonded interactions between the counterions in this study. Non-bonded interactions are determined using the standard functional forms employed by the CHARMM forcefield[1,2] as they are implemented into the LAMMPS MD package[3], in which the nonbond potential energy is determined from the sum of the van der Waals potential energy term (which here is modelled with a Lennard-Jones functional form) and a Coulomb term to model the electrostatic interactions. The only unique thing in the CHARMM forcefield is the use of a shifting function which is used as follows:

$$U_{\text{nonbond}}(r) = \begin{cases} U_{\text{LJ}}(r) + U_{\text{Coul}}(r), & r < r_{\text{in}} \\ S(r)(U_{\text{LJ}}(r) + U_{\text{Coul}}(r)), & r_{\text{in}} < r < r_{\text{out}} \\ 0, & r > r_{\text{out}} \end{cases} \tag{1}$$

where the Lennard-Jones interaction is of the standard 12-6 form:

$$U_{\text{LJ}}(r) = 4\epsilon\left[\left(\frac{\sigma}{r}\right)^{12} - \left(\frac{\sigma}{r}\right)^{6}\right], \tag{2}$$

the electrostatic interactions are modeled with the standard Coulomb term:

$$U_{\text{Coul}}(r) = \frac{Cq_1q_2}{\epsilon r}, \tag{3}$$

and $S(r)$ is a shifting function that is used to smoothly ramp the potential energy and forces to zero for interactions with a distance between the inner and outer cutoff values (r) which were set to $r_{\text{in}} = 10$ Å and $r_{\text{out}} = 12$ Å

[0a] *Theory & Simulation of Condensed Matter Group, Department of Physics, Strand Campus, King's College London, Strand, London WC2R 2LS, England. E-mail: chris.lorenz@kcl.ac.uk*

[0b] *Pharmaceutical Biophysics Group, Institute of Pharmaceutical Science, King's College London, Franklin-Wilkins Building, 150 Stamford Street, London SE1 9NH, England.*

[0c] *Departament de Fisica i Enginyeria Nuclear, Escola Tècnica Superior d'Enginyeria Industrial de Barcelona (ETSEIB), Universitat Politecnica de Catalunya, 08028 Barcelona, Catalonia, Spain.*

respectively within the CHARMM forcefield:

$$S(r) = \frac{[r_{\text{out}}^2 - r^2]^2 [r_{\text{out}}^2 + 2r^2 - 3r_{\text{in}}^2]}{[r_{\text{out}}^2 - r_{\text{in}}^2]^3} \tag{4}$$

where ϵ is the characteristic interaction energy and σ is a characteristic interaction distance, specifically the value of r where the curve intercepts the x-axis. One value for σ and ϵ is provided per atom type, as shown in Table 1, and inter-type interactions are calculated using the arithmetic mean of σ ($\sigma_{\text{ij}} = (\sigma_{\text{i}} + \sigma_{\text{j}})/2$) and the geometric mean of the well-depths ($\epsilon_{\text{ij}} = \sqrt{\epsilon_{\text{i}}\epsilon_{\text{j}}}$).

2 Instructive images of monolayers

Fig. 1 shows a snapshot of the configuration that was used in all of the simulations reported here. In these systems, the two surfactant monolayers, each monolayer composed of 100 DS$^-$ molecules, are separated by a water slab ~ 60 Å thick. While not shown in Fig. 1, the z-dimension of the actual simulation box included $\sim$ 100 Å of vacuum above and below the top and bottom monolayers, respectively. This simulation set-up allows us to gather twice the information about the relevant interactions with a modest additional computational cost.

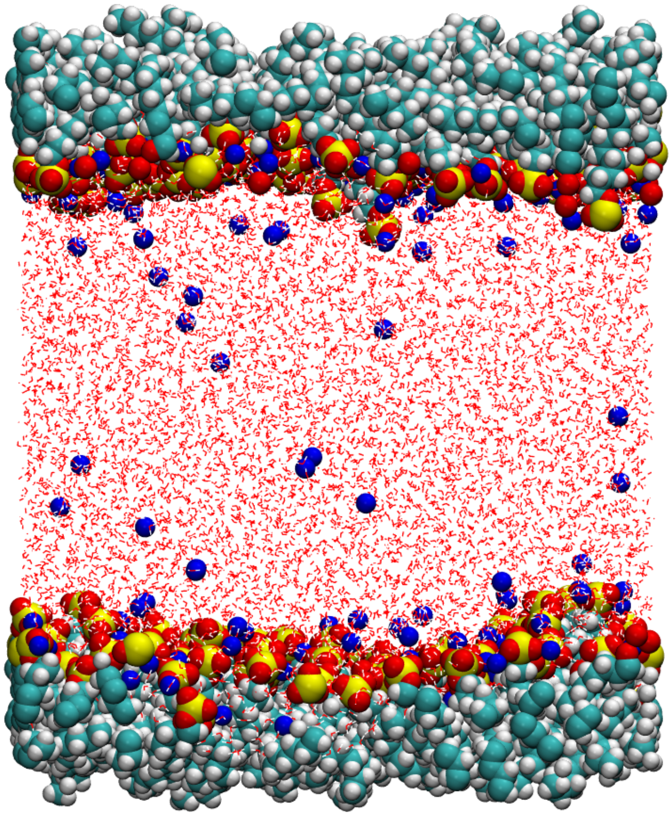

Figure 1: Snapshot of the simulated configuration for the SDS system. The colours cyan, grey, red, yellow and blue are used to represent the elements: carbon, hydrogen, oxygen, sulphur and sodium respectively.

3 Molecular axis sets

Fig. 2 shows the molecular axis sets which were placed on the surfactant, water and ammonium molecules and were used to construct the spatial density maps and to investigate the molecular orientation of water molecules (via the Euler angles) in a specific region around the DS$^-$ headgroups. The axis sets are constituted of 4 pseudoatoms. These pseudoatoms can be placed by using the centre of mass position of a selection of atoms, or alternatively, they can be placed as a cross product of two vectors. This is very useful because the axes must be orthogonal to each other. Note that a slightly different set of molecular axes were used to construct the bivariate probability plots as a function of $cos(\theta_{cm})$ and ϕ_{cm} presented in the main article. The alternate frames of reference presented the results in a clearer way.

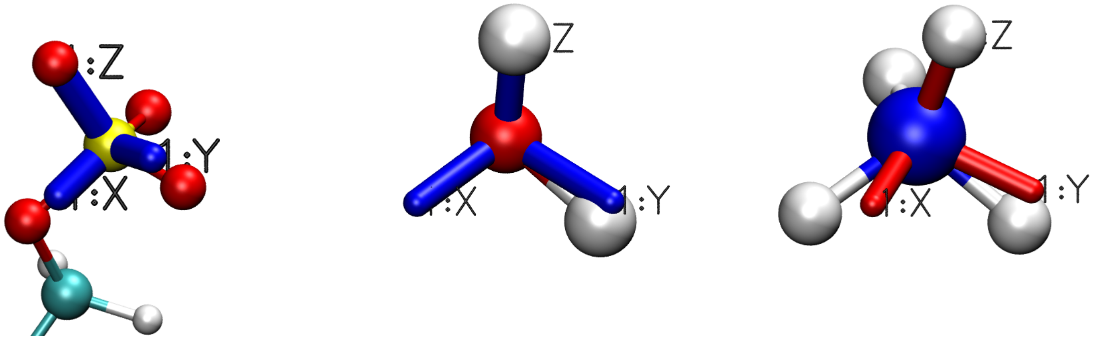

(a) DS^- (b) H_2O (c) NH_4^+

Figure 2: Molecular axes that were used to construct the SDMs and study the orientations of molecules for the (a) dodecyl sulfate headgroup, (b) the water molecule and the NH_4^+ counterions. The axes for the dodecyl sulfate headgroup and the water molecules are shown in blue. The axes for the NH_4^+ ions are shown in red rather than blue so as not to clash with the blue nitrogen atom.

4 Radial Distribution Functions

Fig. 3 shows the various radial distribution functions referred to in the article. These were constructed by counting the number of a given atomic species within spherical shells of width 0.1 Å of a reference atomic species for every pair in every simulation snapshot in the trajectory. These tallies were then divided by the volume of each respective shell: $V = \frac{4}{3}\pi((r+dr)^3 - (r)^3)$.

The nearest neighbor distances and coordination numbers for the $g(r)$ curves are presented in Tables 2 and 3 respectively. The nearest neighbor distances reported in Table 3 are used for calculating the hydration numbers and for determining ion binding and bridging, all of which are reported within the text of the manuscript.

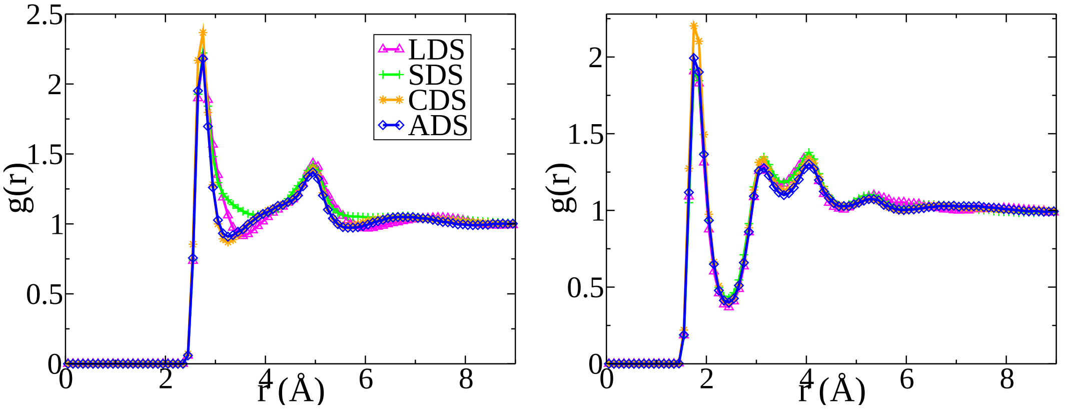

(a) O_{DS}-O_W (b) O_{DS}-H_W

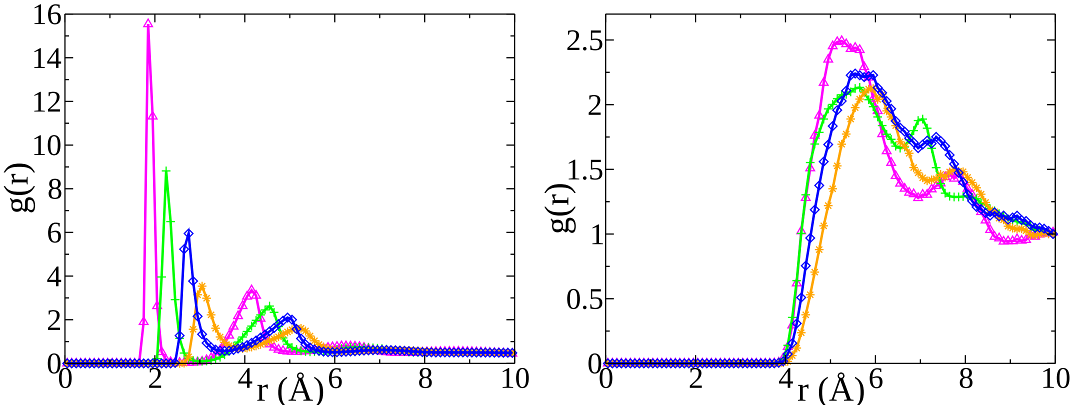

(c) O_{DS}-Ions (d) S_{DS}-S_{DS}

Figure 3: Radial distribution functions ($g(r)$s) for the (a) $O_{DS} - O_W$, (b) $O_{DS} - H_W$, (c) O_{DS} – counterion and (d) $S_{DS} - S_{DS}$ interactions.

Table 2: Nearest neighbor distances from the $g(r)$ curves between the O_{DS} atoms and the different atomic species in the water molecules and counterions.

	LDS	SDS	CDS	ADS
O_W	3.55	3.75	3.25	3.25
Li^+	2.65	-	-	-
Na^+	-	3.05	-	-
Cs^+	-	-	3.95	-
$N_{NH_4^+}$	-	-	-	3.55
$H_{NH_4^+}$	-	-	-	2.35

Table 3: Coordination numbers obtained from the $g(r)$ curves between the O_{DS} atoms and the different atomic species in the water molecules and counterions.

	LDS	SDS	CDS	ADS
O_W	3.31	4.25	2.23	0.43
Li^+	0.30	-	-	-
Na^+	-	0.32	-	-
Cs^+	-	-	0.49	-
$N_{NH_4^+}$	-	-	-	0.47
$H_{NH_4^+}$	-	-	-	0.10

5 Monolayer structure

The structure of the surfactant monolayers is measured in terms of angles formed by different parts of the DS^- molecules. The surfactant chain tilt angle is defined as the angle between the vector formed between the C1 atom (the headgroup carbon atom) and the C12 atom (the carbon atom of the terminal methyl group) and a unit vector in the z-direction. When this angle is zero, the hydrocarbon tail is perfectly aligned with the z-axis and when this angle is 90°, the DS^- molecule is lying in the x-y plane. The top plot in Fig. 4 shows the probability distributions of the surfactant chain tilt angle for all of the simulations.

The surfactant headgroup tilt angle was also investigated for all of the monolayer systems and is defined as the angle between the vector formed between S (the sulphur atom in the SDS head group) and C1 atoms, and the vector formed between C1 and C12 atoms. When this angle is zero, the entire molecule is aligned linearly and when this angle is 90° the head group is oriented such that it is perpendicular to the DS^- hydrocarbon chain. The bottom plot in Fig. 4 shows that the headgroup tilt angle is insensitive to different monovalent counterion species.

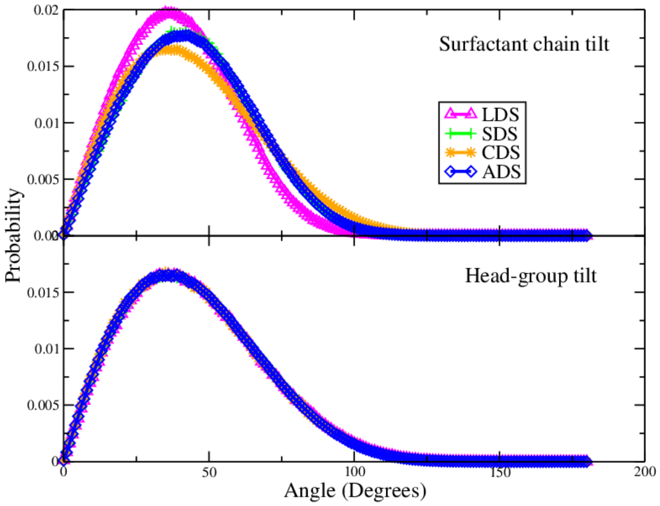

Figure 4: Surfactant chain tilt and head tilt angle distributions. Lithium, sodium, caesium and ammonium are shown in the colours magenta, green, orange and blue respectively.

As we have described in the manuscript, we have identified an intrinisic surface for each monolayer in order to carry out measurements that are a function of the distance from the monolayer surface. Fig. 5 shows the a snapshot of one of the LDS monolayers and the corresponding *intrinsic surface* that we have determined for that configuration. It shows the roughness of the monolayer/water interface and highlights the necessity of using a more sophisticated description of the interface when dealing with such undulations.

Using these intrinsic surfaces as a reference, intrinsic density profiles of the oxygen atoms in water molecules, the oxygen atoms in DS^- headgroups and the first four carbon atoms in the DS^- hydrocarbon chain were determined for all simulations and are shown in Fig. 6. The clearest differences in these profiles are between ADS and the other simulations. The intrinsic density of O_W atoms in the water molecules shows an interfacial peak at the interface for the LDS, SDS and CDS simulations. ADS however shows no such peak due to the strong interactions between ammonium ions and the DS^- head groups displacing interfacial water molecules. The second notable difference between the plots in Fig. 6 is that the ADS O_{DS} atoms show a sharp density peak at $z = 2\text{Å}\dot{T}$his is again likely to be due to the strong salt bridging events between DS^- headgroups and ammonium ions.

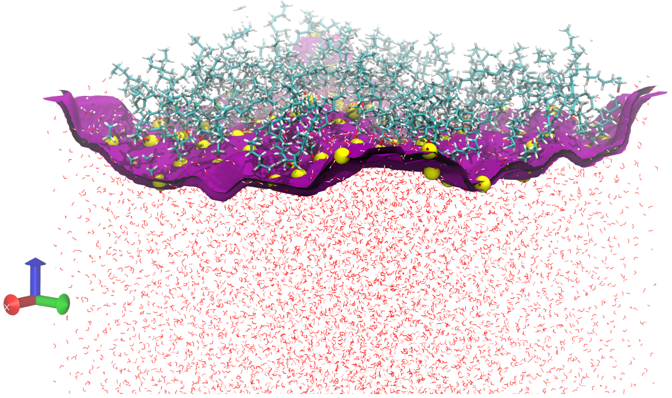

Figure 5: Snapshot of the simulated configuration for the SDS system. The colours cyan, grey, red, yellow and blue are used to represent the elements: carbon, hydrogen, oxygen, sulphur and sodium respectively. The intrinsic surface is depicted in purple.

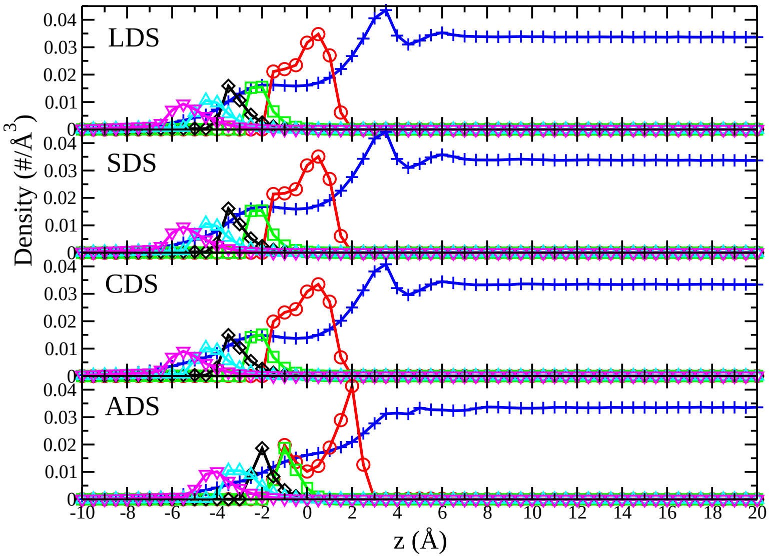

Figure 6: Intrinsic density plots for the monolayer simulations. The colours green, black, cyan and magenta are used to depict the density of DS$^-$ carbons 1-4 respectively. The colours blue and red are used to depict the density of oxygen atoms in water and oxygen atoms in DS$^-$ headgroups respectively.

6 Interfacial water orientation

We were able to study the orientational states of water molecules located within a small region of the O_W SDM, which corresponds to the most probable location to find a water molecule hydrogen bonded to a DS$^-$ head group. Fig. 7 shows the probability of finding a water molecule which is hydrogen bonded to the DS$^-$ head group with it's third principal Euler angle (ψ_{ori}) at a value of ψ. This plot is constructed by taking slices through the trivariate plot of Euler angle states available to the water molecules at this particular point in space, relative to the molecular axis set on DS$^-$ molecules.

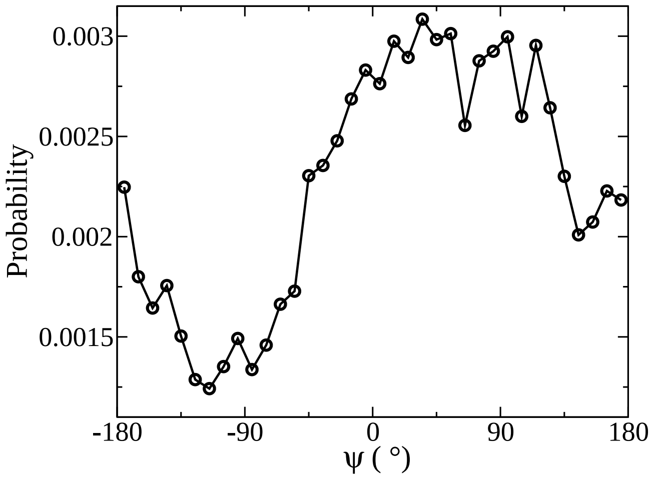

Figure 7: A graph showing the probability of hydrogen bonded water molecule adopting Euler angle ψ for the CDS simulation.

References

[1] K. Vanommeslaeghe, E. Hatcher, C. Acharya, S. Kundu, S. Zhong, J. Shim, E. Darian, O. Guvench, P. Lopes, I. Vorobyov and A. D. Makerell Jr., *J. Comput. Chem.*, 2010, **31**, 671–690.

[2] W. Yu, K. Vanommeslaeghe and A. D. MacKerell Jr., *J. Comput. Chem.*, 2012, **33**, 2451–2468.

[3] S. Plimpton, *J. Comput. Phys.*, 1995, **117**, 1 – 19.